

## Electronic Supplementary Information

# Arsenite Oxyanions Affect CeO<sub>2</sub> Nanoparticle Dissolution and Colloidal Stability

Chelsea W. Neil<sup>1,‡</sup>, Xuanhao Wu<sup>1,†</sup>, Doyoon Kim<sup>1,‡</sup>, Haesung Jung<sup>1,§</sup>, Yanzhe Zhu<sup>1,\*</sup>, Jessica  
R. Ray<sup>1,#</sup>, and Young-Shin Jun<sup>1,\*</sup>

<sup>1</sup>*Department of Energy, Environmental & Chemical Engineering,  
Washington University in St. Louis, St. Louis, MO 63130*

*Address: One Brookings Drive, Campus Box 1180*

*E-mail: ysjun@wustl.edu*

*<http://encl.engineering.wustl.edu/>*

*Submitted: September 2020*

***Environmental Science: Nano***

**\*To Whom Correspondence Should be Addressed**

<sup>‡</sup>Current address: Earth and Environmental Sciences Division, Los Alamos National Laboratory, Los Alamos, NM 87545, USA

<sup>†</sup>Current address: Department of Chemical and Environmental Engineering, Yale University, New Haven, Connecticut, 06510, USA.

<sup>‡</sup>Current address: Department of Civil and Environmental Engineering, Massachusetts Institute of Technology, Cambridge, MA 02139, USA

<sup>§</sup>Current address: School of Civil, Environmental and Chemical Engineering, Changwon National University, Changwon-si, Gyeongsangnam-do, 51140, Republic of Korea

<sup>\*</sup>Current address: Environmental Science & Engineering, California Institute of Technology, Pasadena, CA 91125

<sup>#</sup>Current address: Department of Civil & Environmental Engineering, University of Washington, Seattle, WA 98195

Summary: Total 8 Pages, including 6 Figures

## S1. Effects of dissolved oxygen on the CeO<sub>2</sub> nanoparticle (NP) and arsenite system.

To determine potential effects of dissolved oxygen on the CeO<sub>2</sub> NP and arsenite system, settling tests were conducted outside of the anaerobic chamber, using deionized (DI) water whose oxygen content was equilibrated with the atmosphere. The settling trends of CeO<sub>2</sub> NPs for this system are shown in Figure S1. Settling over the first 8 hours was very similar for the aerobic systems and anaerobic systems, with only the 10<sup>-4</sup> M As<sup>3+</sup> system undergoing significant settling (Figure S1A). Particle size and zeta potential data also showed that the largest size and the lowest zeta potential were in the 10<sup>-4</sup> M As<sup>3+</sup> system, similar to measured values for the anaerobic system. Based on these results, very limited oxidation of aqueous arsenite ions by dissolved oxygen was expected.

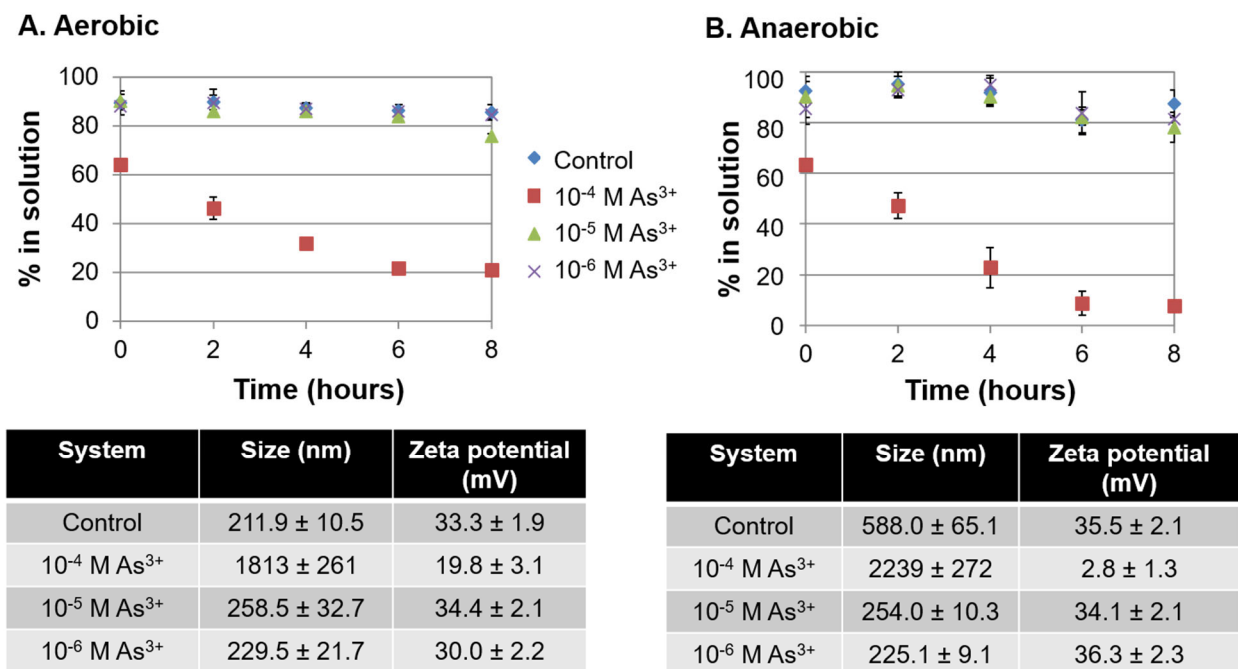
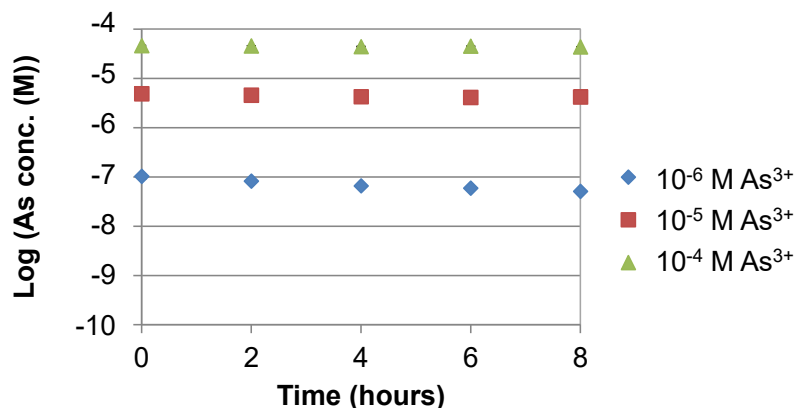


**Figure S1.** Settling trends of CeO<sub>2</sub> NPs for (A) aerobic and (B) anaerobic arsenite systems. Particle size and zeta potential for CeO<sub>2</sub> NP aggregates were measured using Dynamic Light Scattering (DLS).

### A. Anaerobic



### B. Aerobic

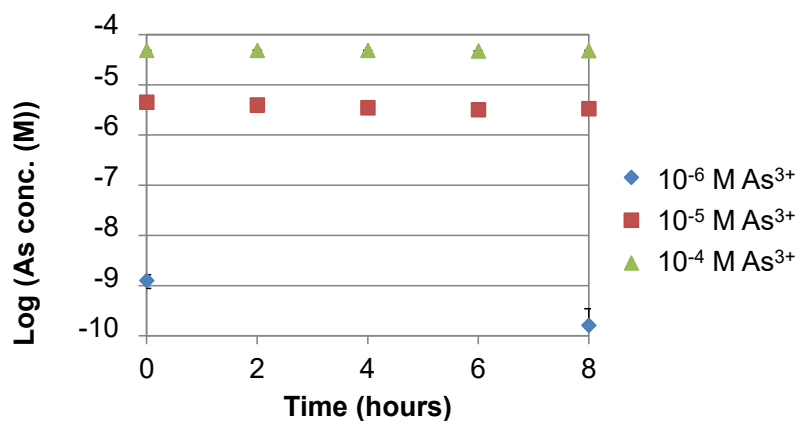


**Figure S2.** Aqueous total arsenic concentrations in (A) anaerobic and (B) aerobic systems. The results are from three replicates, and the error bars are smaller than the size of the symbols. Note that concentrations at 2, 4, and 6 hours in the aerobic system were below the detection limit.

However, when the concentrations of arsenic in the anaerobic and aerobic systems were measured over the 8 hour reaction period (Figure S2), the concentrations were much lower in the 10<sup>-6</sup> M As<sup>3+</sup> system for the aerobic case, in many cases falling below the detection limit for the instrument (Figure S2B, 2, 4, and 6 hours). This finding indicates that oxygen does impact these systems over the first 8 hours of reaction, potentially by oxidizing As<sup>3+</sup> to As<sup>5+</sup>. As<sup>5+</sup> is expected to be less mobile and more easily sorbed at pH 5 because it has a negative charge, while the bare CeO<sub>2</sub> NPs

are charged positively. Therefore, the total aqueous As concentration in the aerobic system decreased compared with the anaerobic system.

Settling in the  $10^{-6}$  M  $\text{As}^{3+}$  system was compared with that in the  $10^{-6}$  M  $\text{As}^{5+}$  system, and the settling trends were similar over the first 8 hours of reaction (Figure S3). The similarity further supports our hypothesis that the oxidation of  $\text{As}^{3+}$  to  $\text{As}^{5+}$  in the aerobic system accounts for the different  $\text{As}^{3+}$  concentration trends (in particular, that of  $10^{-6}$  M  $\text{As}^{3+}$  in Figure S2) in anaerobic and aerobic conditions. Moreover, it also accounts for the similar settling trends in anaerobic and aerobic conditions (Figure S1). In other words, while the oxidation of  $\text{As}^{3+}$  decreases the aqueous  $\text{As}^{3+}$  concentrations in the aerobic system, there is no change in settling between the aerobic and anaerobic systems because the settling trends caused by  $10^{-6}$  M  $\text{As}^{3+}$  and  $10^{-6}$  M  $\text{As}^{5+}$  adsorption on  $\text{CeO}_2$  NPs are similar.

Based on these results, it is clear that the presence of oxygen impacted  $\text{As}^{3+}$  in our experimental system, particularly for the lowest concentration of  $10^{-6}$  M. Therefore, to clearly elucidate direct redox interactions between  $\text{As}^{3+}$  and  $\text{CeO}_2$ , further investigations focused only on

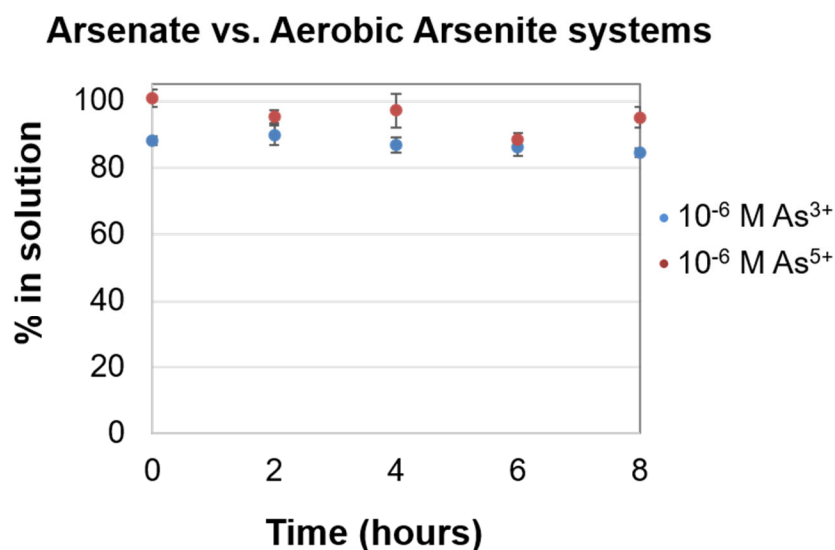
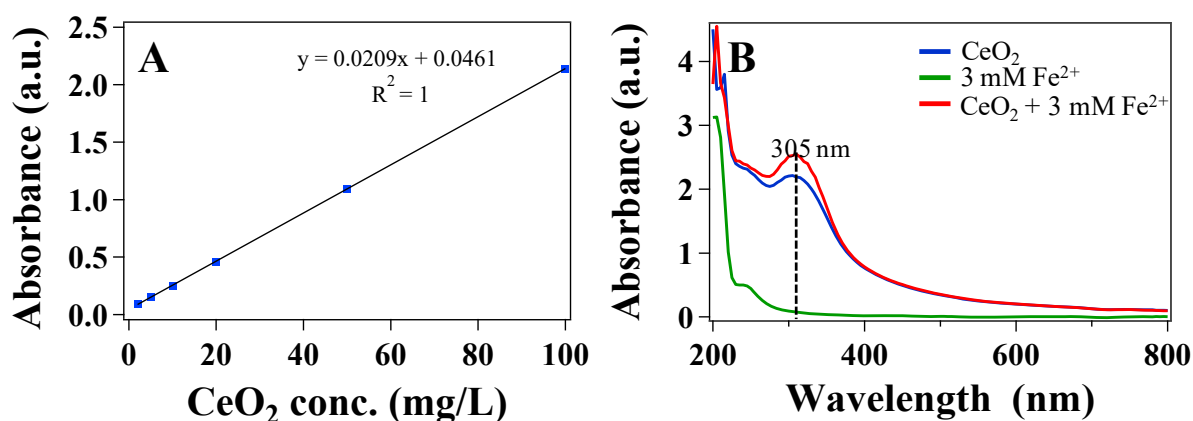


**Figure S3.**  $\text{CeO}_2$  NP settling in the arsenate system under the aerobic condition.

anaerobic systems, in which any observed oxidation of  $\text{As}^{3+}$  had to result from only interactions with  $\text{Ce}^{\text{IV}}\text{O}_2$ .

## S2. UV-Vis calibration for sedimentation experiments

Although there may be contribution from Rayleigh scatter at low absorption wavelengths, the linear relationship between  $\text{CeO}_2$  concentration and the 305 nm wavelength absorption was confirmed over a range of 2–100 mg/L of suspended  $\text{CeO}_2$ .



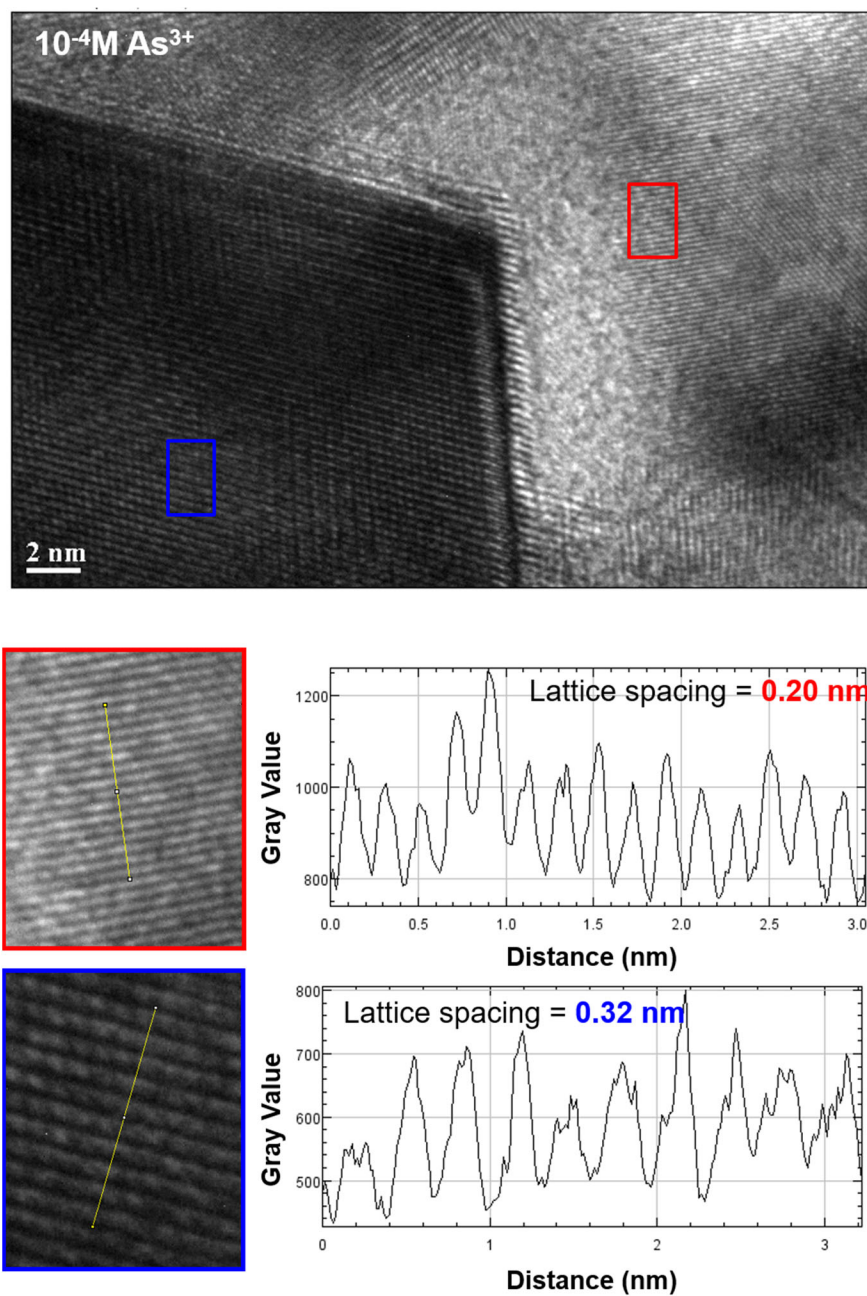
**Figure S4.** (A) Calibration curve for absorbance of 2-100 mg/L  $\text{CeO}_2$  at 305 nm wavelength using UV-vis. (B) UV-Vis spectra of  $\text{CeO}_2$  NP suspension showing absorbance peak at 305 nm.

Figure reprinted with permission from Liu et al.<sup>1</sup>

## S3. Potential secondary phase formation in the $\text{CeO}_2$ NP and arsenite system.

To investigate whether secondary phases formed in the  $\text{CeO}_2$ /arsenite system, we used high resolution transmission electron microscopy (HRTEM, JEOL 2100F, MA). TEM samples were prepared as described in the manuscript. In addition to the large aggregates shown in Figure 2, lattice images were also taken to look for secondary phases in the  $10^{-4}$  M  $\text{As}^{3+}$  system and  $10^{-5}$  M  $\text{As}^{3+}$  system (Figures S5 and S6, respectively). All lattice spacings closely matched those of  $\text{CeO}_2$

nanoparticles, which have lattice spacings of 0.27 nm for (200) facets, 0.31 nm for (111) facets, and 0.21 nm for (511) faces.<sup>2,3</sup> No additional lattice fringes from other solid phases were observed.



**Figure S5.** Lattice fringes of CeO<sub>2</sub> NPs for the 10<sup>-4</sup> M As<sup>3+</sup> system.

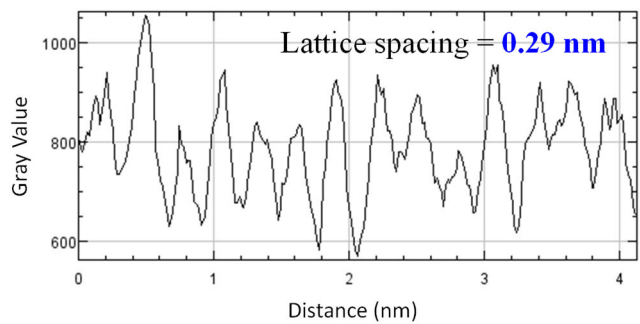
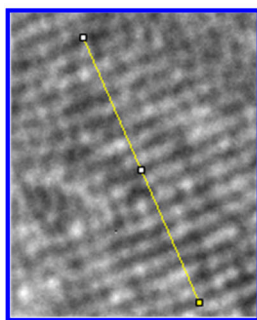
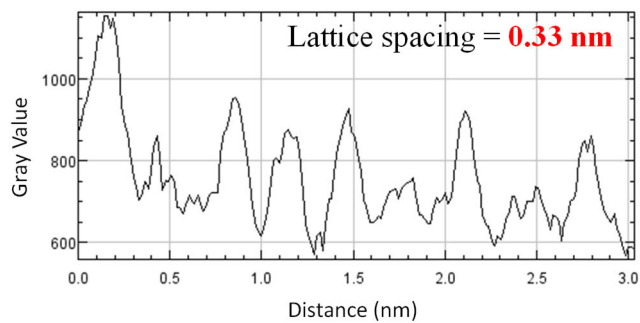
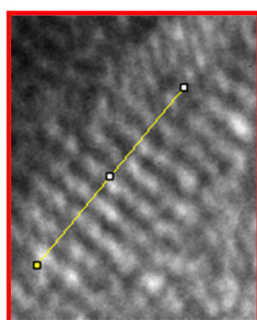
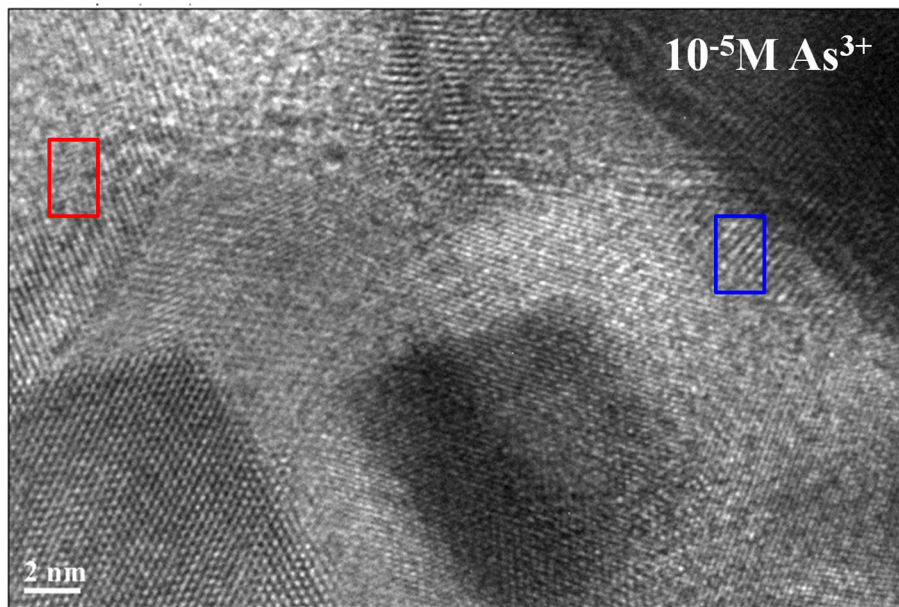


**Figure S6.** Lattice fringes of CeO<sub>2</sub> NPs for the 10<sup>-5</sup> M As<sup>3+</sup> system.

#### **S4. Effects of aggregation on surface area.**

Although the  $10^{-4}$  M  $\text{As}^{3+}$  system has a higher  $\text{As}^{3+}$  concentration, more dissolution occurred in the  $10^{-5}$  M  $\text{As}^{3+}$  system. This dissolution trend indicates that dissolution is related to the amount of exposed surface area in the system, since the  $10^{-4}$  M  $\text{As}^{3+}$  system has a much larger aggregate size than the  $10^{-5}$  M  $\text{As}^{3+}$  system. Where aggregate size is similar in the  $10^{-6}$  M  $\text{As}^{3+}$  and  $10^{-5}$  M  $\text{As}^{3+}$  systems, more dissolution occurs for the higher  $\text{As}^{3+}$  concentration ( $10^{-5}$  M  $\text{As}^{3+}$ ). It is difficult to measure the surface area of aqueous nanoparticle aggregates due to drying effects, which alter the aggregate morphology.<sup>2</sup> However, multiple studies have reported lower surface area for nanoparticle aggregates.<sup>2-4</sup>

#### **References**

1. Liu, X.; Ray, J. R.; Neil, C. W.; Li, Q.; Jun, Y.-S., Enhanced colloidal stability of  $\text{CeO}_2$  nanoparticles by ferrous ions: adsorption, redox reaction, and surface precipitation. *Environ. Sci. Technol.* **2015**, *49* (9), 5476-5483.
2. Gilbert, B.; Ono, R. K.; Ching, K. A.; Kim, C. S., The effects of nanoparticle aggregation processes on aggregate structure and metal uptake. *J Colloid Inter. Sci.* **2009**, *339* (2), 285-295.
3. Braunschweig, J.; Bosch, J.; Meckenstock, R. U., Iron oxide nanoparticles in geomicrobiology: from biogeochemistry to bioremediation. *New Biotechnol.* **2013**, *30* (6), 793-802.
4. Stemig, A. M.; Do, T. A.; Yuwono, V. M.; Arnold, W. A.; Penn, R. L. J. E. S. N., Goethite nanoparticle aggregation: effects of buffers, metal ions, and 4-chloronitrobenzene reduction. *Environ. Sci. Nano* **2014**, *1* (5), 478-487.